INTERNATIONAL JOURNAL OF HYDROGEN ENERGY 39 (2014) 4788–4793

Available online at www.sciencedirect.com

ScienceDirect

journal homepage: www.elsevier.com/locate/he

Enhancing the electrocatalytic water splitting efficiency for amorphous MoS_x

Chang-Lung Hsu [a,b], Yung-Huang Chang [b], Tzu-Yin Chen [b], Chien-Chih Tseng [b], Kung-Hwa Wei [a,**], Lain-Jong Li [b,c,*]

[a] Department of Materials Science and Engineering, National Chiao Tung University, HsinChu 300, Taiwan
[b] Institute of Atomic and Molecular Sciences, Academia Sinica, Taipei 10617, Taiwan
[c] Department of Medical Research, China Medical University Hospital, Taichung, Taiwan

ARTICLE INFO

Article history:
Received 18 November 2013
Received in revised form
7 January 2014
Accepted 13 January 2014
Available online 15 February 2014

Keywords:
Hydrogen evolution reaction
Electrocatalytic reaction
Molybdenum disulfide
Niobium chloride

ABSTRACT

Amorphous molybdenum sulfide (MoS_x) materials have been considered as cheap and promising catalysts for hydrogen evolution reaction (HER). In this contribution, we report that the amorphous MoS_x catalysts prepared by the low temperature thermolysis of the $(NH_4)_2MoS_4$ precursors on carbon clothes (catalyst loading: 3.2 mg/cm^2) exhibit a Tefal slope of 50.5 mV/dec and a high exchange current density of 1.5×10^{-3} mA/cm^2 in 0.5 M H_2SO_4 solutions. Spectroscopic studies of the amorphous MoS_x catalysts show that the increase of HER efficiency is positively correlated to the concentration of S_2^{2-} species, providing strong evidence to support the argument that S_2^{2-} is an active species for electrocatalytic HER. Additionally, the method for preparing catalysts is simple, scalable and applicable for large-scale production.

1. Introduction

The clean energy source such as hydrogen is an ideal energy carrier because there is no carbon dioxide emitted during the combustion process. The production of hydrogen from electrolytic water splitting has gained greater attention than before. Platinum is one of the most efficient catalysts for electrocatalytic hydrogen evolution reaction (HER). However, its high cost and rareness on earth retard the wide applications for HER. Replacing Pt by earth abundant catalysts is critically important for the realization of large-scale HER applications. Among many potential candidates, low cost and earth abundant transition metal dichalcogenides [1–5] such as molybdenum disulfide (MoS_2) and WS_2 have been demonstrated as promising HER catalysts.

Molybdenum disulfide has been used as a solid-state lubricant [6] and the catalysts for hydrodesulfurization (HDS) [7,8], oxygen reduction reaction (ORR) [9] and hydrogen evolution reaction (HER) [10,11]. It has been reported that the high HER activity for the crystalline MoS_2 structures is related to the unsaturated sulfur appearing at the crystal edges [11,12]. It also exhibits relatively good stability in acidic environments [13–19]. However, previous synthetic methods involving ultra-high vacuum processing [11], high-temperature treatment [15,16] or using toxic H_2S for sulfurization [11,15], may not be preferred in large-scale production of catalysts. Recent efforts have been focused on synthesizing highly efficient

* *Corresponding author*. Institute of Atomic and Molecular Sciences, Academia Sinica, Taipei 10617, Taiwan. Tel.: +886 2 23668205.
** *Corresponding author*. Department of Materials Science and Engineering, National Chiao Tung University, HsinChu 300, Taiwan. Tel.: +886 3 57131771.
E-mail addresses: khwei@mail.nctu.edu.tw (K.-H. Wei), lanceli@gate.sinica.edu.tw (L.-J. Li).
0360-3199/$ – see front matter
http://dx.doi.org/10.1016/j.ijhydene.2014.01.090

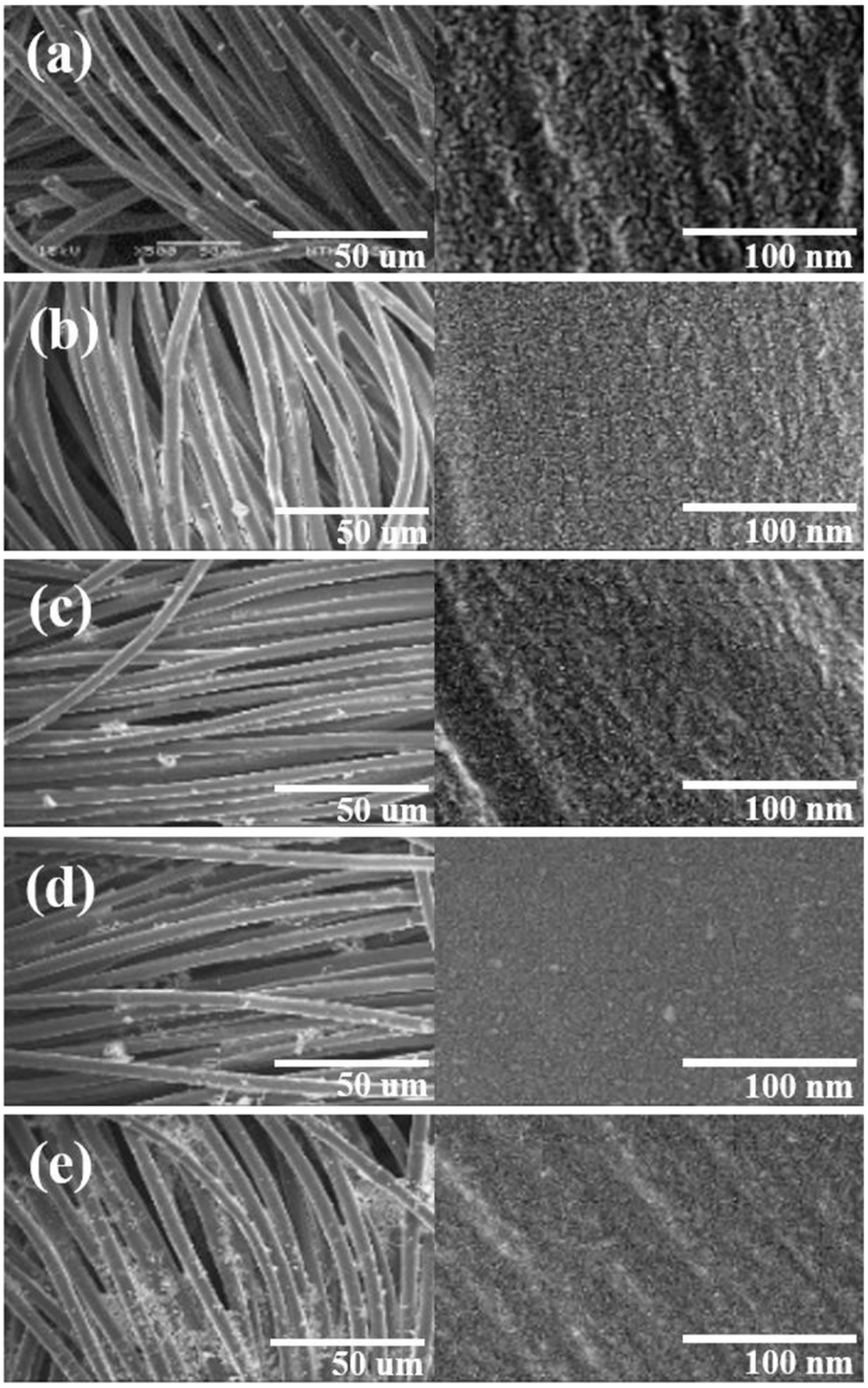

Fig. 1 – SEM images of the amorphous MoS_x catalysts prepared with various $NbCl_5$ solid weight percentages (a) 0 wt% (b) 0.1 wt% (c) 1 wt% (d) 10 wt% (e) 20 wt% Nb.

amorphous molybdenum sulfide catalysts [16,20–22]. Hu et al. have reported the electrochemical method to prepare the amorphous molybdenum sulfide catalysts with impressive HER efficiency [17,22]. The inclusion of Fe, Co, and Ni ions in the amorphous molybdenum sulfide structures further improves the apparent HER activity in acidic environments [21], where the enhancement of HER efficiency has been mainly attributed to the increase in catalyst loading caused by the higher electrochemical growth rate with the presence of Fe, Co, and Ni ions or the enhancement in reactivity of the defect sites [21–25]. The catalytic species in the amorphous MoS_x and the mechanism of the HER efficiency increase in ternary metal sulfide materials still remain as a highly interesting topic.

To further explore study the factors controlling the HER efficiency of ion MoS_x catalysts and to avoid the complication of possible morphological change from electrochemical deposition, we use a simple thermolysis process at 120 °C to prepare the amorphous MoS_x catalysts with the inclusion of various concentrations of $NbCl_5$ (0–20 wt %). It is observed that the incorporation of $NbCl_5$ in the precursor solution results in the enhancement of HER efficiency, and only 1 wt% of $NbCl_5$ is needed to achieve the optimal HER efficiency enhancement (>100%) for MoS_x catalysts. The X-ray photoelectron spectroscopy (XPS) analysis of these catalytic materials reveals that Nb does not bind to MoS_x matrix, suggesting the enhancement is not related to the Nb-doping or Nb-inclusion. Instead, the enhancement in HER efficiency is closely related to structural changes of the MoS_x catalysts, eg. the differences in the content of the S_2^{2-}, Mo^{4+} and Mo^{5+} species in the resulting MoS_x catalysts, caused by the presence of Nb^{5+} in the matrix.

2. Material and method

2.1. Synthesis of catalysts

Ammonium thiomolybdate ($(NH_4)_2MoS_4$, abcr, 99.99%), Niobium chloride ($NbCl_5$, Alfa, 99.95%) and *N*,*N*-dimethylformamide (DMF, Sigma–Aldrich) were used without further purification. A DMF solution was added with desired amount of $(NH_4)_2MoS_4$ and $NbCl_5$ (0.1 wt% ~ 20 wt%), followed by stirring at room temperature for overnight. The carbon clothes were immersed in the solution, baked on a hot-plate at 100 °C for 10 min and annealed at 120 °C in the H_2/Ar environment (H_2:Ar = 20:80; 500 torr) in a CVD furnace to form amorphous MoS_x and Nb-added MoS_x catalysts. We measured the weight of each blank carbon clothes before and after the deposition of different catalysts, where the catalyst loading was obtained as the weight difference divided by the area of each sample.

2.2. Characterization

Chemical bonding structures of the catalysts were determined by X-ray photoelectron spectroscopy (XPS) (Phi 5000) with Mg Kα X-ray source. The energy calibrations were made against to the C 1s peak to eliminate the charging of the sample during analysis. The surface morphology was examined by a field-emission scanning electron microscope (FESEM) (JSM-6500F). Polarization curves were recorded by an AUTOLAB pontentiostat (PGSTAT 302N) with a scan rate of 5 mV/s in a 0.5 M H_2SO_4 solution. A three-electrode configuration using an Ag/AgCl (saturated KCl) electrode as the reference electrode, a graphite rod as the counter electrode, and the MoS_x and Nb-added MoS_x on carbon clothes as working electrodes were adopted for polarization and electrolysis measurements. Electrochemical surface analysis (ESA) was also performed on an AUTOLAB pontentiostat (PGSTAT 302N) at different scan rate of 5, 6, 7, 8, 9, 10 mV/s in a 0.035 M $K_3[Fe(CN)_6]$ solution. A three-electrode configuration is using an Ag/AgCl (saturated KCl) electrode as the reference electrode, Pt as the counter electrode, and the MoS_x/carbon clothes samples as working electrode.

3. Results and discussion

In this contribution, Niobium is selected as the HER promoter since the Niobium-derivatives in the bulk state has been shown to exhibit high activity in hydro–desulfurization reactions [26,27]. The MoS_x-based HER catalysts were prepared by the thermolysis of the $(NH_4)_2MoS_4$ precursors at 120 °C, where the carbon clothes were dipped into a 5 wt% of $(NH_4)_2MoS_4$ in DMF. To tailor the HER efficiency of the MoS_x catalysts, various percentages of $NbCl_5$ from 0.1 wt% to 20 wt % (solid content) were added in the precursor solution. Note that our previous report [28] has shown that the HER performance of the pristine and amorphous MoS_x catalysts synthesized by the thermolysis method is optimal with the synthetic temperature at around 120 °C. Fig. 1(a)–(e) show the scanning electron microscopy (SEM) images of the MoS_x catalysts prepared with the addition of with various percentages of $NbCl_5$ (0 wt%, 0.1 wt% 1 wt%, 10 wt% and 20 wt% of solid weight) on carbon clothes. The carbon fiber diameter is ~10 μm and the surface of the intrinsic MoS_x seems slightly a little bit rougher than $NbCl_5$ added MoS_x systems. The morphology of these samples revealed in SEM looks quite similar. Consistently, the measured electrochemical surface area (ESA) for all these samples does not vary much (in between 1.86 and 1.92 cm^2 as shown in Table 1), which makes the direct comparison of the catalyst HER efficiency easier. Fig. 2(a) shows the polarization curves of these amorphous MoS_x catalysts, where the current is normalized by the geometrical area of the carbon clothes and the HER is performed in a 0.5 M H_2SO_4 solution. At the applied voltage of −0.3 V, it is observed that the HER efficiency increases from the 66.0 mA/cm^2 for pristine MoS_x to the 89.6 mA/cm^2 for the MoS_x incorporating 1 wt% $NbCl_5$. However, the further increase in $NbCl_5$ wt% results in a lower HER efficiency. For better comparison, the current density at the applied

Table 1 – Characterizations of the catalysts prepared in this study, including catalyst loading, XPS, ESA and electrical performance.

$NbCl_5$ solid content in precursor	Catalyst loading (mg/cm^2)	$Mo^{5+}/(Mo^{4+}+Mo^{5+})$ (%)	S_2^{-2}/%	Current density (mA/cm^2)	Current density (A/g)	Tafel slope (mV/dec)	J_0 (mA/cm^2)	ESA (cm^2)
0 wt %	3.2	16.7	31.7	66.0	20.6	50.5	1.5×10^{-3}	1.912
0.1 wt %	2.9	26.9	51.2	81.1	28.1	48.0	1.7×10^{-3}	1.888
1 wt%	3.0	29.1	56.6	89.6	30.1	46.0	3.3×10^{-3}	1.921
10 wt%	2.9	27.1	51.6	84.9	29.1	51.9	2.5×10^{-3}	1.871
20 wt%	3.3	22.0	41.8	81.0	22.6	45.5	2.4×10^{-3}	1.863

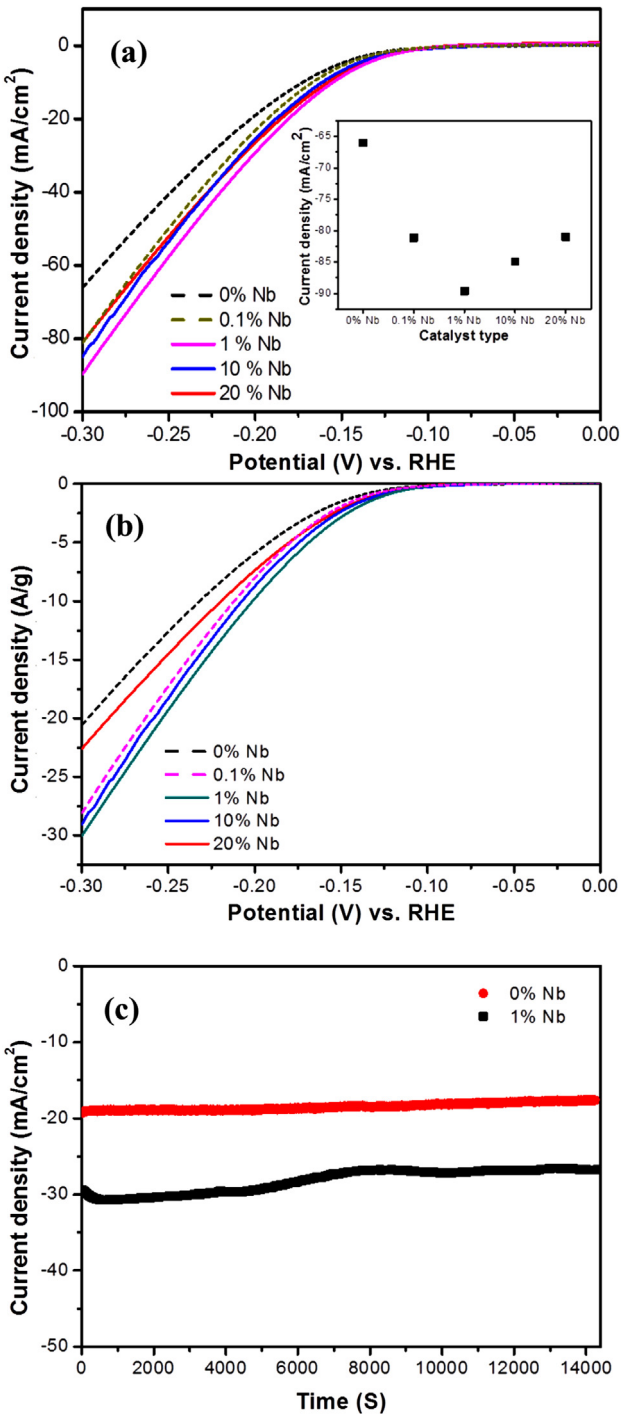

Fig. 2 – The polarization curves of the amorphous MoS_x catalysts. (a) The current is normalized by the geometrical area of the carbon clothes (b) The current is normalized by the loading weight (c) The HER stability of 0 wt% and 1 wt% of $NbCl_5$-addition.

potential of −0.3 V is plotted as a function of $NbCl_5$ wt % in inset of Fig. 2(a). Fig. 2(b) shows the polarization curves normalized by the loading weight of each catalyst and the observed trend is similar to that normalized by the geometrical area (Fig. 2(a)). Consistently, the best HER efficiency is observed for the sample MoS_x with 1 wt% of $NbCl_5$ addition, which value is 30.1 A/g at the applied potential of −0.3 V.

According to classical HER theory, the catalytic performance of electrodes for HER can be described by Tafel relationship (Eq. (1)),

$$\eta = b \ln\left(\frac{i}{i_0}\right) \quad (1)$$

where η is the overpotential, i is the current density, and i_0 is the exchange current density. The Tafel slope b is the measurement of the potential increase required to enhance the resulting current density one order of magnitude, normally used to evaluate the efficiency of the catalytic reaction. The electrical curves (ln i vs. η) for the MoS_x catalysts show good linear relation when the overpotential is between −0.109 V and −0.141 V. The Tafel slope of the intrinsic MoS_x is extracted as 50.5 mV/dec and the exchange current density is 0.15×10^{-2} mA/cm^2. For the 1 wt% $NbCl_5$-added MoS_x, the Tafel slope is improved to 46.0 mV/dec and the exchange current density is as high as 0.33×10^{-2} mA/cm^2. Moreover, the comparison of the catalytic stability between the intrinsic MoS_x and the 1 wt% $NbCl_5$-added MoS_x is shown in Fig. 2(c). At an overpotential of V = −0.2 V, the current density of MoS_x and 1 wt% $NbCl_5$-added MoS_x is 18.9 mA/cm^2 and 27.1 mA/cm^2, respectively, over a period of 3 h. The hydrogen production durability of the 1 wt% Nb-added MoS_x is comparable to that of pristine MoS_x. It is noted that several recent reports have hypothesized that the edges of MoS_2 crystals might be related to the HER reactivity in MoS_x materials [11,12,22]. In this report, all the catalysts are prepared at a low temperature and exhibit no Raman or X-ray diffraction features, suggesting all these materials are amorphous. Hence, alternative explanation is required to interpret our experimental observation. To understand the differences between the pristine and $NbCl_5$-added MoS_x catalysts, XPS was adopted to characterize the chemical bonding structures. Fig. 3 displays the detailed XPS scans for the Mo and S binding energies for these catalysts. The binding energies of 229.2 eV and 232.4 eV are attributed to Mo $3d_{5/2}$ and $3d_{3/2}$ electrons for the Mo^{4+} state in MoS_2 [21,29,30]. The binding energies of Mo $3d_{5/2}$ and $3d_{3/2}$ orbitals observed at 230.0 eV and 233.1 eV are originated from the Mo^{5+} state of Mo_2S_5 [21,29,30]. Note that the peak at 226.7 eV is assigned to S 2s [21,29,30]. The two peaks at 161.7 eV and 162.8 eV are the signature of the S $2p_{1/2}$ and $2p_{3/2}$ electrons of S^{2-} [21,29,30]. The 163.2 eV and 164.3 eV peaks correspond to the S $2p_{1/2}$ and $2p_{3/2}$ orbital of S_2^{2-} [21,29,30]. Surprisingly, the binding energies of Nb are hardly detectable for all samples. Only very weak $3d_{5/2}$ and $3d_{3/2}$ peaks for the Nb^{5+} state are observed at 207.7 eV and 210.5 eV [31] for the sample added with 20 wt% $NbCl_5$ (see Supporting Figure S1). These results point out that the Nb ions do not chemically bind to the MoS_x matrix although the Nb and the HER efficiency enhancement is related to the structural difference of the MoS_x catalysts. Table 1 summarizes the characterization results for these catalysts, including catalyst loading, XPS, surface area and electrical performance.

Several recent reports have speculated that the unsaturated sulfur atoms such as S_2^{2-} could be related to the HER activity [28,32]. We can estimate the relative content of S_2^{2-} and S^{2-} by comparing the area sum of the S_2^{2-} doublet peaks

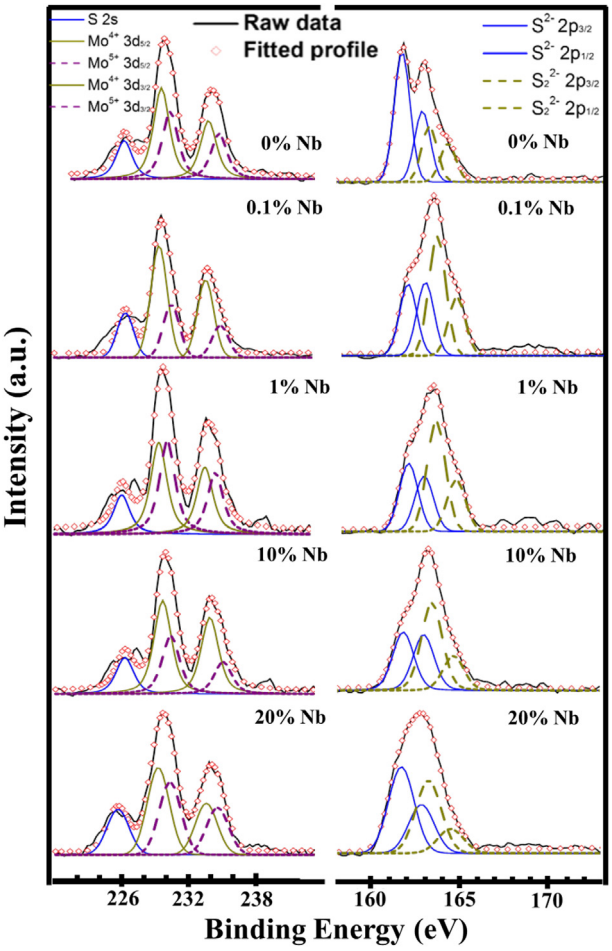

Fig. 3 – XPS spectra of the amorphous MoS_x catalysts.

(163.2 eV and 164.3 eV) and that of the S^{2-} doublet peaks (161.7 eV and 162.8 eV). The content of the S_2^{2-}, estimated from the ratio $S_2^{2-}/(S_2^{2-} + S^{2-})$, for each catalyst is shown in Table 1. Note that the MoS_x catalyst with 1 wt% of $NbCl_5$ addition contains the highest S_2^{2-} ratio (56.6%). Fig. 4 shows that the measured HER performance of these catalysts exhibits nice exhibits nice correlation to the S_2^{2-} content, where the catalyst

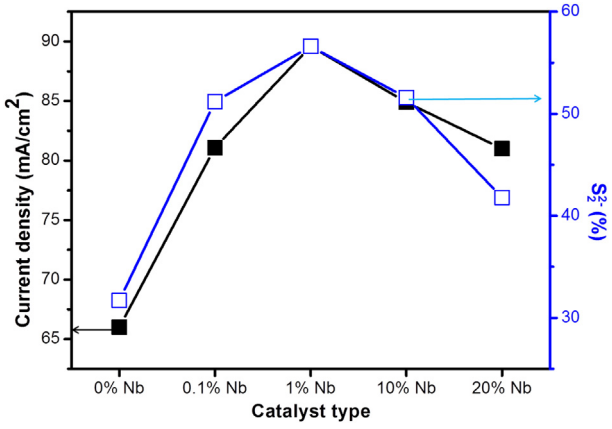

Fig. 4 – HER performance of these catalysts is positively correlated to the S_2^{2-} content in the chemical composition.

with a higher S_2^{2-} content displays a larger HER current density. It is also noted that the content of Mo^{5+} (estimated by $Mo^{5+}/(Mo^{4+} + Mo^{5+})$ in XPS) is positively correlated to the S_2^{2-} content (Table 1). These observations provide strong evidence to support the argument that S_2^{2-} is the active species for electrocatalytic HER in MoS_x systems. The XPS results suggest that the Nb atoms do not chemically bind to the MoS_x matrix. However, the observed enhancement in HER with the $NbCl_5$ addition is reproducible. Although it is not clear how the $NbCl_5$ inclusion affects the formation of various MoS_x structures at this stage, the formation of various MoS_x structures could involve the dynamic competition between the reaction of Nb^{5+} with S^{2-} and its decomposition which warrants more future studies.

4. Conclusions

A fast, low-temperature and scalable thermolysis process is used to produce amorphous MoS_x catalysts for HER. The addition of $NbCl_5$ in the precursor solution is able to enhance the HER efficiency of obtained MoS_x catalysts. Noticeably, the inclusion of only 1 wt% $NbCl_5$ in the MoS_x catalysts results in a 100% enhancement in exchange current density and a lowering of the Tafel slope to 46 mV/dec. The positive correlation between the HER performance and S_2^{2-} quantities strongly suggests that S_2^{2-} is the active species for electrocatalytic HER in MoS_x systems.

Acknowledgments

This research was mainly supported by Academia Sinica (IAMS and Nano program) and National Science Council Taiwan (102-2119-M-001-005-MY3 and 99-2738-M-001-001).

Appendix A. Supplementary data

Supplementary data related to this article can be found at http://dx.doi.org/10.1016/j.ijhydene.2014.01.090

REFERENCES

[1] Coleman JN, Lotya M, O'Neill A, Bergin SD, King PJ, Khan U, et al. Two-Dimensional nanosheets produced by liquid exfoliation of layered materials. Science 2011;331:568–71.
[2] Chhowalla M, Shin HS, Eda G, Li LJ, Loh KP, Zhang H. The chemistry of two-dimensional layered transition metal dichalcogenide nanosheets. Nat Chem 2013;5:263–75.
[3] Song X, Hu J, Zeng H. Two-dimensional semiconductors: recent progress and future perspectives. J Mater Chem C 2013;1:2952–69.
[4] Li H, Lu G, Wang YL, Yin ZY, Cong CX, He QY, et al. Mechanical exfoliation and characterization of single- and few-layer nanosheets of WSe_2, TaS_2, and $TaSe_2$. Small 2013;9:1974–81.
[5] Komsa HP, Kotakoski J, Kurasch S, Lehtinen O, Kaiser U, Krasheninnikov AV. Two-Dimensional transition metal

dichalcogenides under electron irradiation: defect production and doping. Phys Rev Lett 2012;109:035503.
[6] Chhowalla M, Amaratunga GAJ. Thin films of fullerene-like MoS_2 nanoparticles with ultra-low friction and wear. Nature 2000;407:164–7.
[7] Prins R, Debeer VHJ, Somorjai GA. Structure and function of the catalyst and the promoter in Co—Mo hydrodesulfurization. Catal Catal Rev Sci Eng 1989;31:1–41.
[8] Salmeron M, Somorjai GA, Wold A, Chianelli R, Liang KS. The adsorption and binding of thiophene, butene and H_2S on the basal plane of MoS_2 single crystals. Chem Phys Lett 1982;90:105–7.
[9] Ahmed SM, Gerischer H. Influence of crystal surface orientation on redox reactions at semiconducting MoS_2. Electrochim Acta 1979;24:705–11.
[10] Hinnemann B, Moses PG, Bonde J, Jørgensen KP, Nielsen JH, Horch S, et al. Biomimetic hydrogen evolution: MoS_2 nanoparticles as catalyst for hydrogen evolution. J Am Chem Soc 2005;127:5308–9.
[11] Jaramillo TF, Jørgensen KP, Bonde J, Nielsen JH, Horch S, Chorkendorff I. Identification of active edge sites for electrochemical H_2 evolution from MoS_2 nanocatalysts. Science 2007;317:100–2.
[12] Xie JF, Zhang H, Li S, Wang RX, Sun X, Zhou M, et al. Defect-rich MoS_2 ultrathin nanosheets with additional active edge sites for enhanced electrocatalytic hydrogen evolution. Adv Mater; 2013. http://dx.doi.org/10.1002/adma.201302685.
[13] Jaramillo TF, Bonde J, Zhang JD, Ooi BL, Andersson K, Ulstrup J, et al. Hydrogen evolution on supported incomplete cubane-type $[Mo_3S_4]^{4+}$electrocatalysts. J Phys Chem C 2008;112:17492–8.
[14] Bonde J, Moses PG, Jaramillo TF, Norskov JK, Chorkendorff I. Hydrogen evolution on nano-particulate transition metal sulphides. Faraday Discuss 2008;140:219–31.
[15] Chen ZB, Cummins D, Reinecke BN, Clark E, Sunkara MK, Jaramillo TF. Core–shell MoO_3–MoS_2 nanowires for hydrogen evolution: a functional design for electrocatalytic materials. Nano Lett 2011;11:4168–75.
[16] Li YG, Wang HL, Xie LM, Liang YY, Hong GS, Dai HJ. MoS_2 nanoparticles grown on graphene: an advanced catalyst for the hydrogen evolution reaction. J Am Chem Soc 2011;133:7296–9.
[17] Merki D, Fierro S, Vrubel H, Hu XL. Amorphous molybdenum sulfide films as catalysts for electrochemical hydrogen production in water. Chem Sci 2011;2:1262–7.
[18] Merki D, Hu XL. Recent developments of molybdenum and tungsten sulfides as hydrogenevolution catalysts. Energy Environ Sci 2011;4:3878–88.
[19] Laursen AB, Kegnaes S, Dahl S, Chorkendorff I. Molybdenum sulfides—efficient and viable materials for electro – and photoelectrocatalytic hydrogen evolution. Energy Environ Sci 2012;5:5577–91.
[20] Tang ML, Grauer DC, Lassalle-Kaiser B, Yachandra VK, Amirav L, Long JR, et al. Structural and electronic study of an amorphous MoS_3 hydrogen-generation catalyst on a quantum-controlled photosensitizer. Angew Chem Int Ed 2011;50:10203–7.
[21] Merki D, Vrubel H, Rovelli L, Fierro S, Hu XL. Fe, Co, and Ni ions promote the catalytic activity of amorphous molybdenum sulfide films for hydrogen evolution. Chem Sci 2012;3:2515–25.
[22] Vrubel H, Merki D, Hu XL. Hydrogen evolution catalyzed by MoS_3 and MoS_2 particles. Energy Environ Sci 2012;5:6136–44.
[23] Lauritsen JV, Helveg S, Lægsgaard E, Stensgaard I, Clausen BS, Topsøe H, et al. Atomic-scale structure of Co–Mo–S nanoclusters in hydrotreating catalysts. J Catal 2001;197:1–5.
[24] Sun MY, Nelson AE, Adjaye J. On the incorporation of nickel and cobalt into MoS_2-edge structures. J Catal 2004;226:32–40.
[25] Raybaud P, Hafner J, Kresse G, Kasztelany S, Toulhoat H. Structure, energetics, and electronic properties of the surface of a promoted MoS_2 catalyst: an ab initio local density functional study. J Catal 2000;190:128–43.
[26] Geantet C, Afonso J, Breysse M, Allali N, Danot M. Niobium sulfides as catalysts for hydrotreating reactions. Catal Today 1996;28:23–30.
[27] Allali N, Leblanc A, Danot M, Geantet C, Vrinat M, Breysse M. Catalytic properties of pure and Ni doped niobium sulfide catalysts for hydrodesulfurization. Catal Today 1996;27:137–44.
[28] Chang YH, Lin CT, Chen TY, Hsu CL, Zhang W, Wei KH, et al. Highly efficient electrocatalytic hydrogen production by MoS_x grown on graphene-protected 3-dimentional Ni foams. Adv Mater 2013;25:756–60.
[29] Weber Th, Muijsers JC, van Wolput JHMC, Verhagen CPJ, Niemantsverdriet JW. Facile synthesis of low crystalline MoS_2 nanosheet-coated CNTs for enhanced hydrogen evolution reaction. J Phys Chem 1996;100:14144–50.
[30] Wang HW, Skeldon P, Thompson GE. XPS studies of MoS_2 formation from ammonium tetrathiomolybdate solutions. Surf Coat Technol 1997;91:200–7.
[31] Izawa K, Ida S, Unal U, Yamaguchi T, Kang JH, Choy JH, et al. A new approach for the synthesis of layered niobium sulfide and restacking route of NbS_2 nanosheet. J Solid State Chem 2008;181:319–24.
[32] Chen TY, Chang YH, Hsu CL, Wei KH, Chiang CY, Li LJ. Comparative study on MoS_2 and WS_2 for electrocatalytic water splitting. Int J Hydrogen Energy 2013;38:12302–9.